THE EFFECTIVENESS OF USING GPR TO MONITOR CHANGES IN SOIL WATER CONTENT IN CLAYEY FLOODPLAIN SOILS DUE TO RAIN EVENTS BEFORE STREAM MODIFICATIONS

Jon Algeo & Robert W Jacob, Dept. of Geology, Bucknell University, Lewisburg PA, 17837

1. Abstract

Greater infiltration of natural rain water into the subsurface decreases the amount of rapid discharge to streams. The Miller Run watershed in Lewisburg, PA experiences significant rapid discharge during rainfall events due to impervious surfaces, naturally clayey soil and modification of the Miller Run channel. In this study, the effectiveness of using ground-penetrating radar (GPR) common mid-point soundings (CMPs) to monitor soil water content (SWC) is evaluated in the clay-rich environment of the watershed in order to monitor planned engineering modifications to the floodplain. Using non-invasive geophysical methods ensures that the research won't modify the environment being studied. We used several geophysical methods in order to determine the general distribution of clay and determine the subsurface structure. EM-38 was used to locate the area where the conductivity was highest. Subsurface layer thicknesses were assessed using DC resistivity based upon electric properties.

After significant storm events totaling at least two inches of rainfall, 200 MHz GPR was used to collect a series of CMP data. The arrival time for a shallow reflection was used to determine the velocity of the GPR signal. For the September storm, the velocity changes from .062 m/ns before the storm, to 0.054 m/ns after the storm, to 0.059 m/ns five days after the storm. The depth estimate for the reflection based on the reflection analysis is 0.22 m ± 0.05 m. This implies that GPR can be used to monitor changes in soil water content (SWC) in the clay soils within the Miller Run watershed.

2. Introduction

The depth to which a GPR signal penetrates is controlled by a number of factors. An important factor is the percentage of clay contained in the targeted medium. Clay, which has a high electric conductivity as well as a high absorptive capacity for water, causes significant attenuation in GPR signal (Doolittle et al, 2007). Other researchers have shown that the classic Topp relationship relating dielectric constant to soil water content can be used to determine soil water content from GPR velocity (Jacob, 2006, and Hubbard & Grote, 2002). These researchers performed their experiments in sandy or loamy environments. My research focuses on determining the effectiveness of using GPR in a clay-rich environment for the purpose of monitoring changes in SWC in response to rainfall events. Noninvasive methods are used in an effort to avoid disturbing the system being studied. The location of my research is the floodplain of the Miller Run, which cuts across Bucknell University campus in Lewisburg, PA, the location of which is shown in Figure 1.

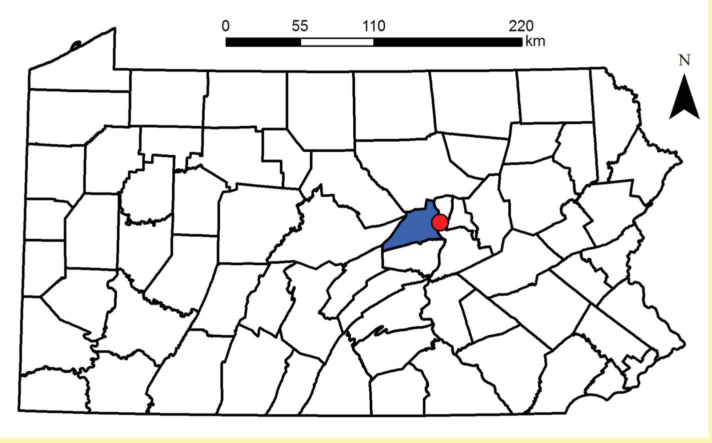

Figure 1. Location of the field site within Lewisburg, Union County, Pennsylvania, United States. Union county is shaded blue, and the red dot represents Lewisburg, PA.

3. Electromagnetics Background

A Geonics EM-38-MK2 unit was selected to perform an EM grid survey due to it's shallow depth of penetration. The expected attenuation of the GPR means that we are only interested in the very shallow subsurface. Clay has one of the highest electric conductivities of any subsurface material, at approximately .01 mS/m (Burger, 2006). We therefore interpreted the highest conductivity area of the floodplain as the area with the most clay. The EM grid (Figures 4 and 5) is 20 meters wide by 91 meters long. The lines are spaced a half meter apart. The device was operated in horizontal dipole mode to target the shallowest segment of the subsurface. An area for further geophysical investigation (Figure 5) was selected based on the data, targeting one of the highest conductivity areas in the field.

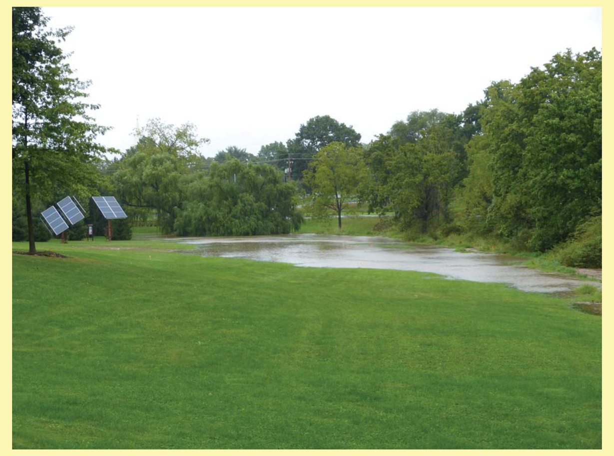

Figure 2. Targeted floodplain during a storm

Figure 3. EM-38_MK2 being carried in horizontal dipole mode

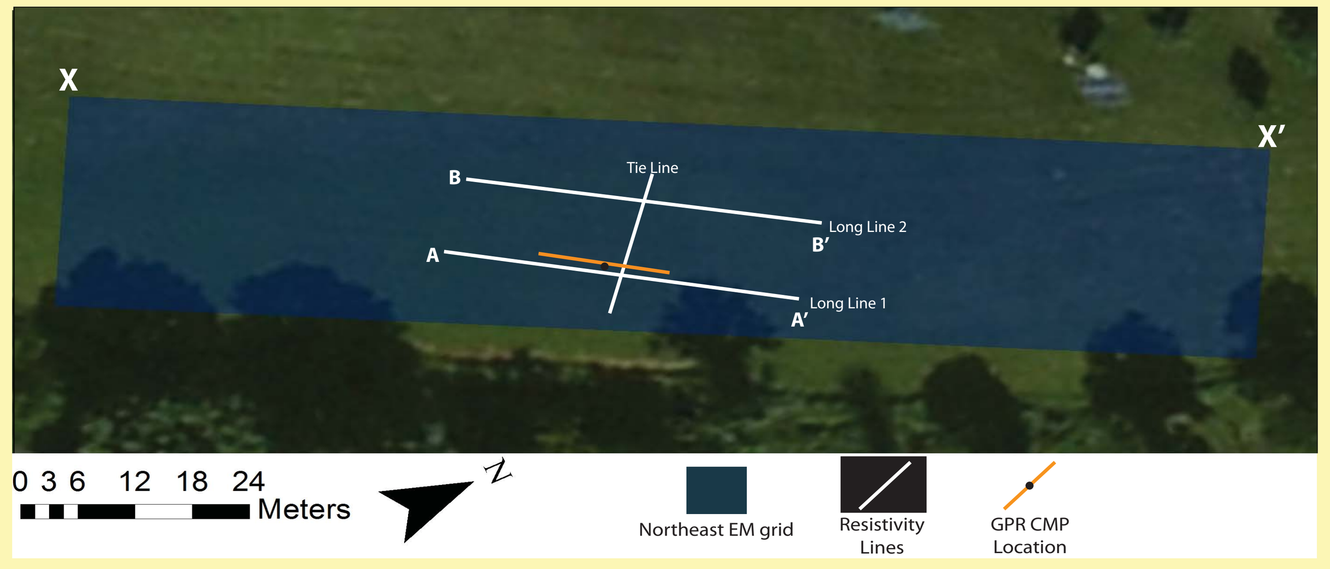

Figure 4. Location of the various geophysical surveys performed for the study.

4. Electromagnetics Data Analysis

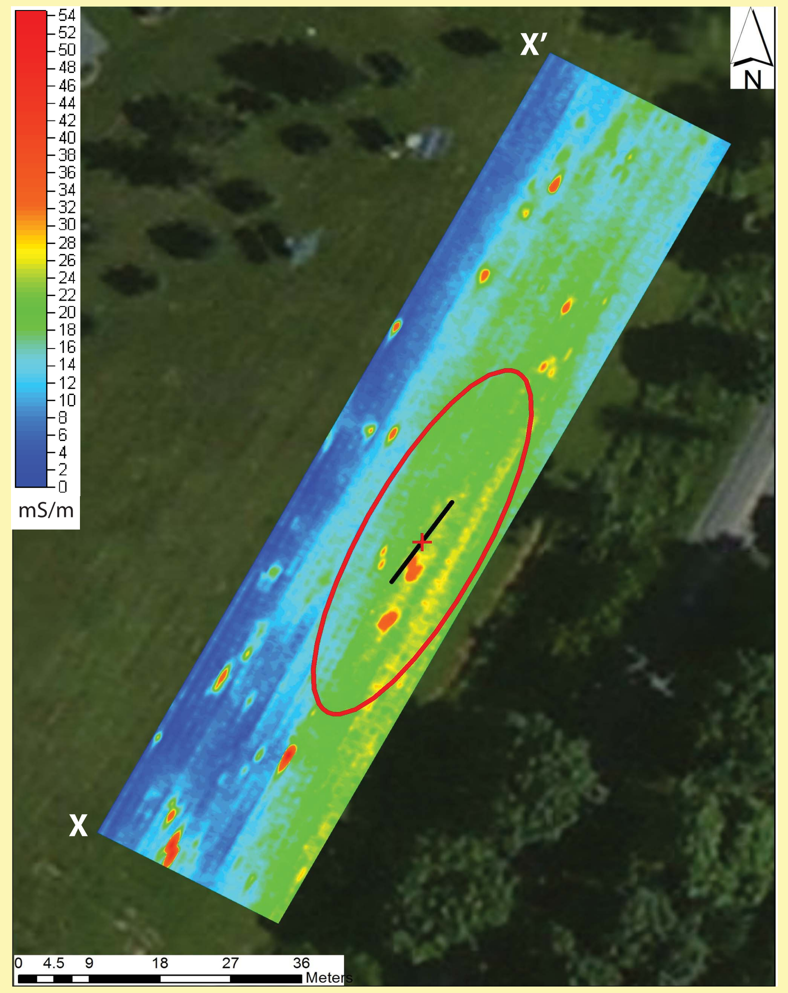

Figure 5. Data collected by EM-38-MK2. One meter coil separation, horizontal dipole. Targeted area is circled. GPR CMP located at red plus.

The EM-38-MK2 data showed significant variation in conductivity within the floodplain. A location was chosen for a GPR CMP (Figure 5) based upon:

1) The high conductivity of the location, suggestive of clay subsurface (~30 mS/m)

2) The flat topography, allowing for infiltration of rainwater

3) The lateral extent of the area, capable of accomodating resistivity lines.

5. DC Resistivity Background

The Sting/Swift multielectrode system measured the resistivity of the subsurface along three lines in my targeted study area (Figure 4). Resistivity was used to characterize the layers in the subsurface by detecting at what depth significant changes in resistivity occur (Michot et al, 2003). The two lines running from southwest to northeast had one meter a-spacing and were 28 meters in length. The tie line running from northwest to southeast was 14 meters long, as it has a half meter a-spacing. The electrodes were placed into the ground, attempting to minimize their penetration depth. A contact resistance test provided data on how well electricity was being transmitted into the ground via the electrodes. Salt water was applied as per manufacturer instruction to the ground at the base of the electrodes when the contact resistance was over 800 ohm*meters.

Figure 6. Left, DC resistivity line taking measurements.

Figure 7. Right, AGI Sting R1 and Swift Smart Electrode System

6. DC Resistivity Data Analysis

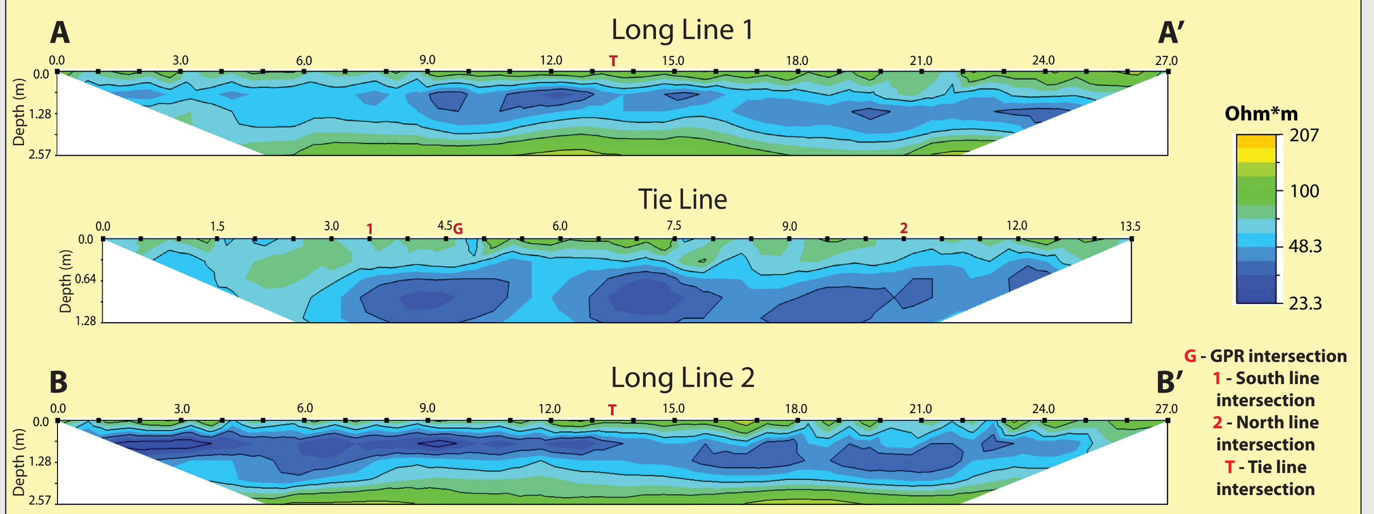

Figure 8. Results of DC Resistivity lines.

Discussion

1) The Tie Line and Long Line 1 indicate the presence of an interface at approximately 50 cm, where the resistivity switches from approximately 100 ohm*m to 50 ohm*m. This can be interpreted as a clay layer.

2) Long Line 2 shows the interface closer to the surface, at approximately 40 cm depth. This implies the interface dips towards Miller Run

3) The layer below this, based on the local geology, is expected to be a soil derived from shale bedrock

7. GPR Background

The Sensors and Software Pulse EKKO Pro with 200 MHz antennas took CMP measurements at the selected location. Van Overmeeren et al (1997) also used GPR to determine SWC. The researchers use the relationship $\mathbf{c/\sqrt{(\varepsilon_r)}}$ to determine the dielectric constant from GPR wave velocity. Following this, they applied the Topp relationship (Topp et al, 1980) between SWC and the dielectric constant:

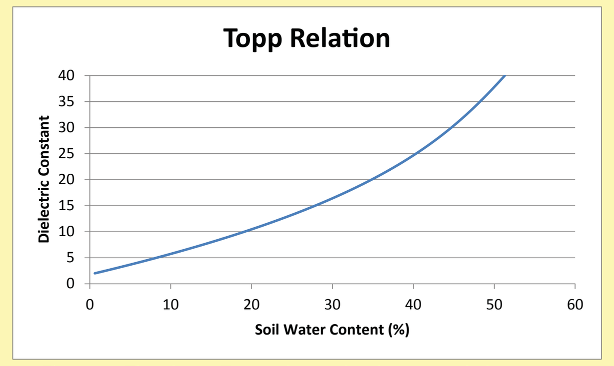

Figure 9. The classic Topp relationship between dielectric constant and SWC. Garambois et al (2001) were able to accurately map SWC in a sandy soil using this method.

Stoffregen et al (2002) investigated the accuracy of the GPR method for estimating SWC by comparing GPR estimates of SWC to estimates from a lysimeter. Their intent was to provide an alternate method to TDR, which involves invasively installing probes in the subsurface, and is expensive in terms of both time and money. Stoffregen et al (2002) determined the velocity of the GPR wave by taking the known depth to the reflecting interface, which was the base of the lysimeter. They then used the relationship $\mathbf{\varepsilon_r=(ct/2d)^2}$ where ε_r is the dielectric constant, c is the velocity of radar waves in air, d is depth to reflector, and t is two-way traveltime of the GPR wave, to determine the relative dielectric constant of any material. The researchers found that, with the high frequency GPR waves they were using, in a sandy soil the SWC could be monitored with an accuracy of .01 m^3/m^3 . I applied the aforementioned relationship to estimate the SWC from my GPR CMPs and then compared the results to soil cores.

8. GPR Analysis

Picks and Forward Models

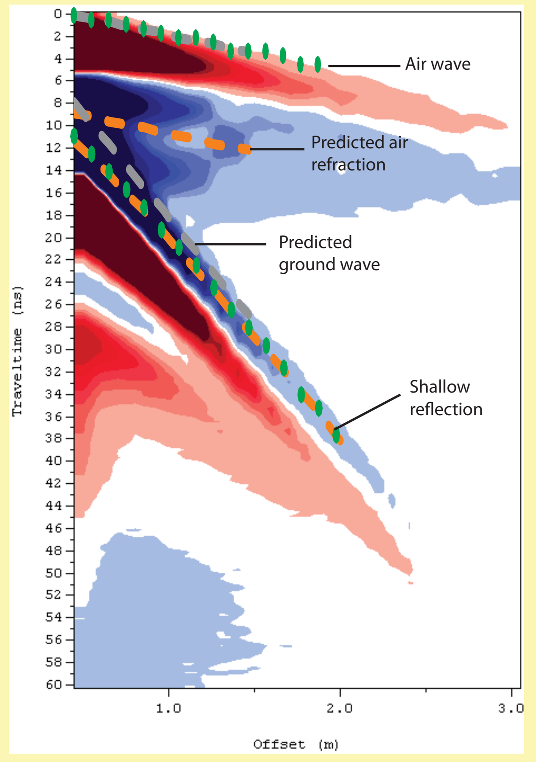

Figure 10. Overlay of picks (filled blue circles) with forward models of various phases (dashed lines). Picks were shifted to correspond with the air wave intersecting 0 ns traveltime at 0 m offset.

Interpretation as Shallow Reflection

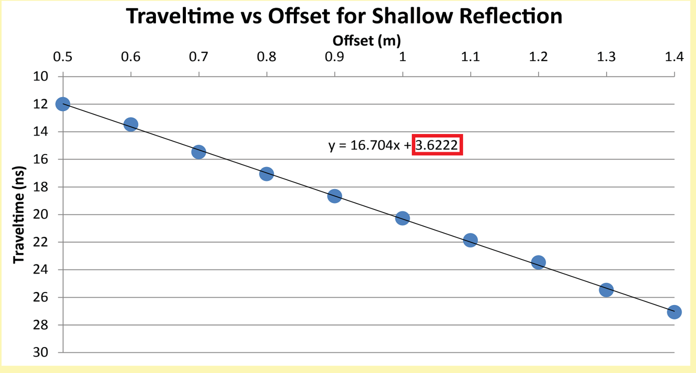

Figure 11. A ground wave at 0 meter offset will have a traveltime of 0 ns. The picks of the shallow reflection show an intercept of 3.6 ns. Therefore, the signal cannot be interpreted as a direct wave.

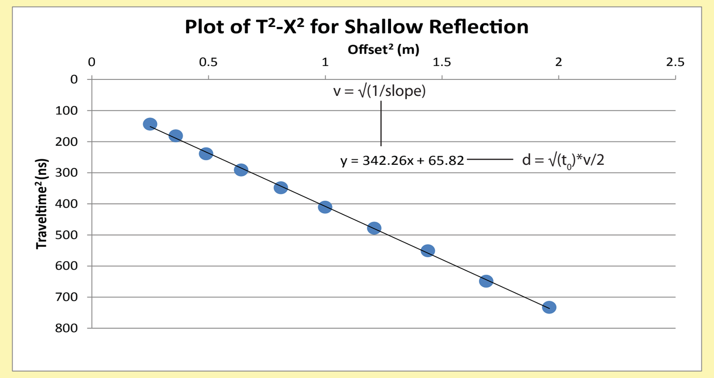

Figure 12. The picks of the shallow reflection in T^2-X^2 space were analyzed to provide a depth estimate to the reflector and velocity of the subsurface above the reflector.

September 19, 2012, Pre-storm / September 21, 2012, Post-storm

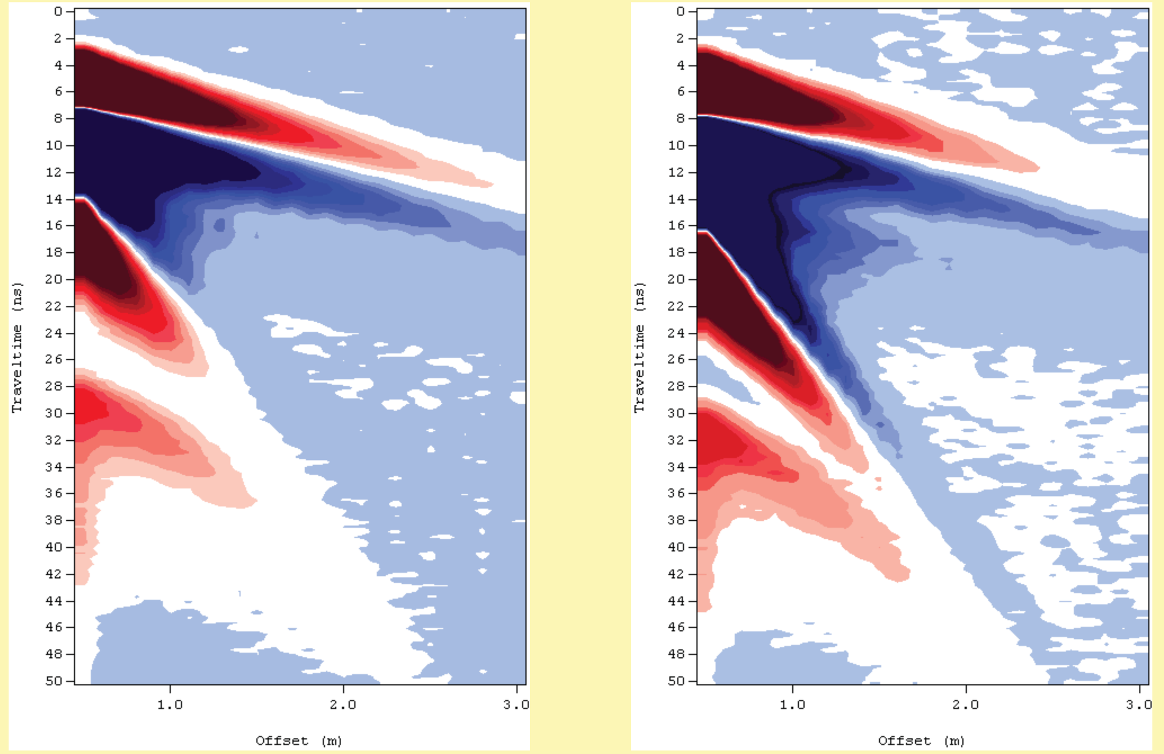

Figure 13. These two figures represent two CMPs, one taken before a rainstorm of 2.19" of rain, and one taken after the storm. There are two noteworthy changes. The arrival of the two interpreted reflections is later after the rainstorm, as would be expected. Additionally, more signal enters the ground after the rainstorm. This leads to a less pronounced airwave and a more pronounced pair of reflections, as well as a stronger signal for what appears to be a refracted air wave.

9. Results

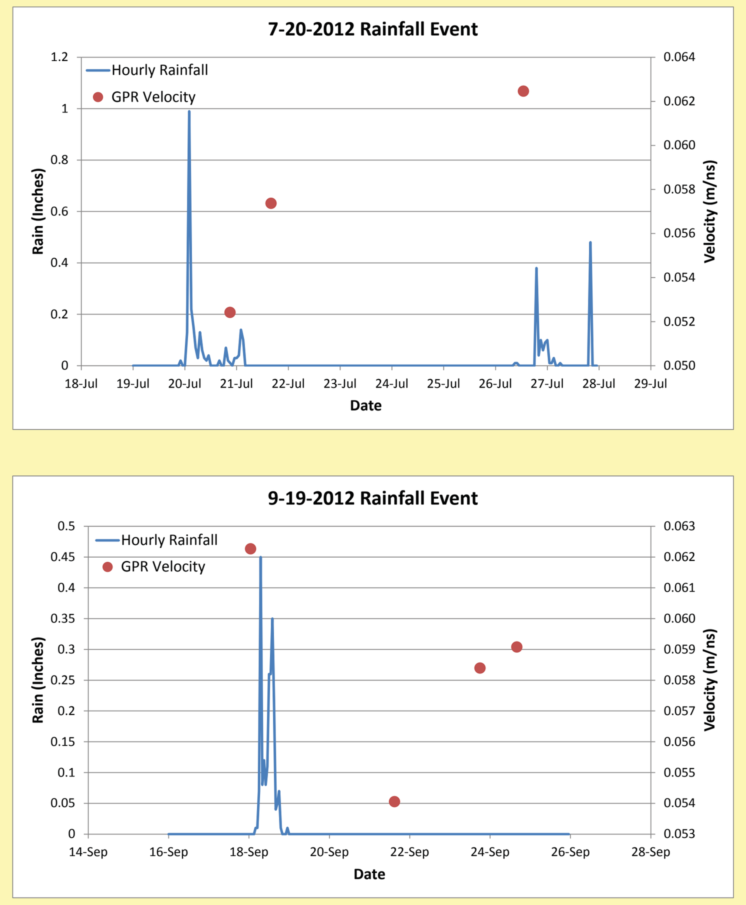

Figure 14. Hourly rainfall measurements for the two storms with calculated GPR velocities on secondary axis.

Direct Measurement and Repeatability

Figure 15. Soil core gravimetric and volumetric analysis was used as a direct measurement to estimate SWC. 2 cm diameter soil cores were taken 2 meters southeast of the GPR CMP. The cores were individually bagged, weighed, and dried in an oven at 60 degrees celcius for two weeks. They were then reweighed and SWC was calculated.

Auger Repeatability Measurements

Date	Location	Gravimetric	Volumetric
10/2/2012	West	30.4%	40.2%
10/2/2012	Middle	31.7%	42.0%
10/2/2012	East	31.5%	41.7%

Table 1. Test of auger repeatability. Three soil cores were taken concurrently and analyzed. The SWC measurements agree well.

GPR Repeatability Measurements

Date	GPR Velocity (m/ns)	Depth (m)	GPR SWC
10/2/2012	0.052	0.233	46.5%
10/2/2012	0.053	0.252	45.9%

Table 2. Test of GPR repeatability. Two GPR CMPs were taken one after the other and analyzed. The results suggest excellent repeatability.

GPR Rainstorm Measurements

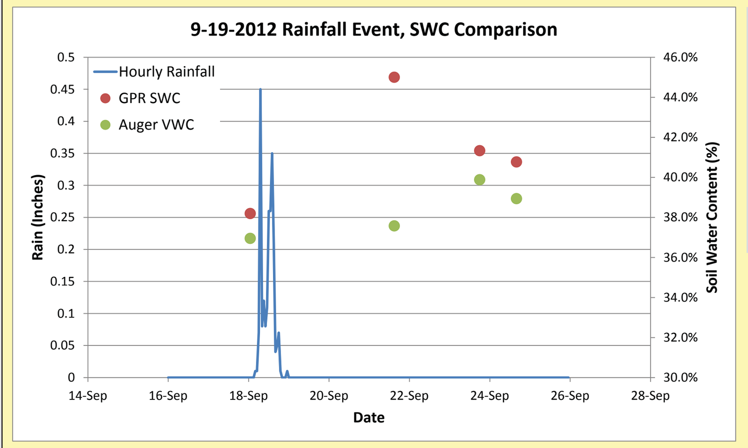

Date	GPR Velocity (m/ns)	Depth (m)	GPR SWC	Gravimetric	Volumetric
7/20/12	0.052	0.235	46.42%		
7/21/12	0.057	0.267	42.18%		
7/26/12	0.062	0.229	38.04%		
9/18/12	0.062	0.168	38.19%	27.9%	36.9%
9/21/12	0.054	0.219	44.99%	28.4%	37.6%
9/23/12	0.058	0.210	41.33%	30.1%	39.9%
9/24/12	0.059	0.208	40.77%	29.4%	38.9%

Table 3. Above, calculated GPR velocity, depth to reflector, and SWC based upon GPR, gravimetric analysis, and volumetric analysis for the two storms.

Figure 16. Left, Comparison of GPR SWC estimate and auger core volumetric SWC

10. Conclusions

1) GPR shows significant potential for measuring changes in SWC in a clay subsurface. Despite the attenuation caused by clay-rich materials, the 200 MHz GPR CMP detected two reflections

2) The primary reflection, approximately 22 cm deep, was used to calculate SWC via the Topp relationship

3) The measurements showed the expected relationship between time, rain amount, and velocity

4) The SWC was confirmed by the auger core measurements

Bibliography

Burger, Henry Robert, Anne F. Sheehan, Craig H. Jones, and Henry Robert Burger. Introduction to Applied Geophysics: Exploring the Shallow Subsurface. New York: W.W. Norton, 2006. Print.

Doolittle, J.a., F.e. Minzenmayer, S.w. Waltman, E.c. Benham, J.w. Tuttle, and S.d. Peaslee. "Ground-penetrating Radar Soil Suitability Map of the Conterminous United States." Geoderma 141.3-4 (2007): 416-21.

Garambois, Stéphane, Pascale Sénéchal, and Hervé Perroud. "On the Use of Combined Geophysical Methods to Assess Water Content and Water Conductivity of Near-surface Formations." Journal of Hydrology 259.1-4 (2002): 32-48. Print.

Hubbard, S. Grote, K. and Rubin, Y., Estimation of near-subsurface water content using high frequency GPR ground wave data, Leading Edge of Exploration, Society of Exploration Geophysics, VJ. 21, No. 6, 552-559, 2002.

Jacob, Robert W. Precision Ground Penetrating Radar Measurements to Monitor Hydrologic Processes Occurring in Unsaturated Subsurface Material. Diss. Brown University, 2006.

Michot, D., Benderitter, Y., Dorigny, A., Nicoullaud, B., King, D. and Tabbagh, A. (2003). Spatial and temporal monitoring of soil water content with an irrigated corn crop cover using surface electrical resistivity tomography. Water Resources Research 39(5): doi: 10.1029/2002WR001581. issn: 0043-1397.

Stoffregen, H., T. Zenker, and G. Wessolek. "Accuracy of Soil Water Content Measurements Using Ground Penetrating Radar: Comparison of Ground Penetrating Radar and Lysimeter Data." Journal of Hydrology 267.3-4 (2002): 201-06. Print.

Topp, G. C., J. L. Davis, and A. P. Annan (1980), Electromagnetic determination of soil water content: Measurements in coaxial transmission lines, Water Resour. Res., 16(3), 574–582, doi:10.1029/WR016i003p00574.

Van Overmeeren, R.A., Sariowan, S.V. and Gehrels, J.C., 1997, Ground penetrating radar for determining volumetric soil water content: results of comparative measurements at two sites: Journal of Hydrology, 197, 316-338.

Acknowledgements

The McKenna Foundation for their funding of my summer research
Kyle Kissock, Bucknell '13 and Jason Muhlbauer, Bucknell '13 for insightful peer review
Brad Jordan and Carilee Dill of the Bucknell Geology Department for all the ways in which they facilitated the research
Becky Joseph, Bucknell '14 for assisting in data collection